

## Shape Anisotropy and Optical Birefringence Measurements of Dry and Swollen Liquid Single Crystal Elastomers

Yusril YUSUF<sup>1\*</sup>, Naoki MINAMI<sup>1</sup>, Shohei YAMAGUCHI<sup>1</sup>,  
Dong-Uk CHO<sup>1</sup>, P. E. CLADIS<sup>2</sup>, Helmut R. BRAND<sup>3</sup>,  
Heino FINKELMANN<sup>4</sup>, and Shoichi KAI<sup>1,5†</sup>

<sup>1</sup>Department of Applied Quantum Physics and Nuclear Engineering,  
Graduate School of Engineering, Kyushu University, Fukuoka 812-8581

<sup>2</sup>Advanced Liquid Crystal Technologies, POB 1314, Summit, NJ 07902, U.S.A.

<sup>3</sup>Theoretische Physik III, Universität Bayreuth, 95440 Bayreuth, Germany

<sup>4</sup>Makromolekulare Chemie, Universität Freiburg, 79104 Freiburg, Germany

<sup>5</sup>Department of Applied Physics, Faculty of Engineering, and Department of Life Engineering,  
Graduate School of Systems Life Sciences, Kyushu University, Fukuoka 812-8581

(Received March 23, 2007; accepted May 1, 2007; published July 10, 2007)

We study the relation between the shape anisotropy changes,  $\Delta\alpha$ , and the optical birefringence,  $\Delta n$ , of dry and swollen rigid bi-functionally (8.0 mol %, 8A2) and flexible tri-functionally [5 mol % (5V3) and 7 mol % (7V3)] cross-linked liquid single crystal elastomers (LSCEs) as a function of temperature. 4-*n*-pentyl-4-cyanobiphenyl (5CB) is used as the solvent. Plotting  $\Delta\alpha$  as a function of  $\Delta n$ , a linear dependence is observed for all LSCE samples. This indicates that  $\Delta\alpha$  results from the liquid crystal ordering. The largest  $\Delta\alpha$  ( $\sim 0.2$  at  $T = 30^\circ\text{C}$ ) is observed in dry 8A2, which has a large frozen-in orientational order (FOO). The swollen samples show much smaller  $\Delta\alpha$ ,  $\sim 0.03\text{--}0.05$ , because of a smaller modulus elasticity after the swelling process.

KEYWORDS: liquid crystal elastomer, thermomechanical effects  
DOI: [10.1143/JPSJ.76.073602](https://doi.org/10.1143/JPSJ.76.073602)

The various properties of liquid crystal elastomers (LCEs) have attracted considerable attention from researchers.<sup>1–6</sup> The most remarkable property of liquid single crystal elastomers (LSCE), the monodomain LCEs, is their ability to significantly change their shape at the nematic to isotropic phase transition. This thermo-mechanical deformation of LSCEs has received considerable attention as a candidate for soft artificial muscles.<sup>5–8</sup>

LSCEs consist of the cross-linked polymer chain networks and liquid crystalline ordering of side chain mesogenic groups.<sup>2–6</sup> This network is synthesized in two steps by the addition of cross-linking agents to the polymer chains. The second cross-linking step is carried out under the influence of a sufficiently large strain, giving rise to a uniform director orientation denoted by a unit pseudo-vector,  $\hat{\mathbf{n}}$ .<sup>2,3</sup> Thus, a unique direction for long range orientational order is frozen in [hereafter called the frozen-in orientational order (FOO)].<sup>9</sup> The other factors influencing FOO are the cross-linking density and the functionality of the crosslinker. These are as strongly responsible for their thermomechanical effects as the dielectric anisotropy of mesogens for the electromechanical effects. It is important to clarify the contribution of these factors in order to obtain more functional LSCE materials.

To understand the effect of cross-linkers on swelling and thermo-mechanical properties, we focus our investigation on LSCEs with two different cross-linkers and different concentrations, i.e., the rigid bi-functional (8.0 mol %) and the flexible tri-functional (5 and 7 mol %) cross-linkers. Previously, we have reported the thermo-mechanical properties of the bi-functionally cross-linked LSCEs (8A2)<sup>10,11</sup> and the tri-functionally cross-linked LSCEs (V3-LSCE).<sup>12,13</sup>

Here, we demonstrate the correlations between macroscopic shape changes and the LSCE orientational order as a function of temperature.

The LSCE materials studied here were originally developed by one of the present authors (H.F.). The chemical structures of the LSCE are shown in Fig. 1. The polymer backbone is a poly(methyl hydrosiloxane) [Fig. 1(a)]. The pendant mesogenic groups comprise 4-(3-butenoxy)-benzoic acid-(4-methoxy)phenyl attached to the backbone via a hydrosilation reaction [Fig. 1(b)]. These networks are chemically crosslinked with the rigid bi-functional [poly(dimethylsiloxane) with terminal vinyl groups] and the flexible tri-functional (1,3,5-tris-undec-10-enoxy-benzene) cross-linkers [Fig. 1(c)]. The cross-linking concentrations are 8.0 mol % for the bi-functionally cross-linked LSCE (8A2) and 5 mol % (5V3) and 7 mol % (7V3) for the tri-functionally cross-linked LSCE.

Two types of rectangular LSCEs samples with different bulk director orientation with respect to  $\hat{\mathbf{n}}$  were investigated, i.e., planar and homeotropic orientations. The thickness of the samples is  $\sim 400\ \mu\text{m}$  with an area of  $\sim 0.7 \times 0.5\ \text{mm}^2$ . The sample is observed using a microscope (Nikon) equipped with a hot stage (Mettler Toledo FP90 Central Processor) as a temperature controller. The image at each temperature is photographed during the heating and cooling processes within a range of 30 to 120 °C, and the scan rate of the temperature is about 0.5 K/min.

The intensity of transmitted light during the heating process is observed using a polarizing microscope equipped with a photodetector and a He–Ne laser as a light source.

In the present study, we obtain the following physical variables: anisotropy of the birefringence,  $\Delta n$ , and of the shape changes,  $\Delta\alpha$ . As is well known from fundamental liquid crystal theory,  $\Delta n$  is proportional to the nematic order parameter,  $S$ :

\*E-mail: yusuf@athena.ap.kyushu-u.ac.jp

†E-mail: kaitap@mbox.nc.kyushu-u.ac.jp

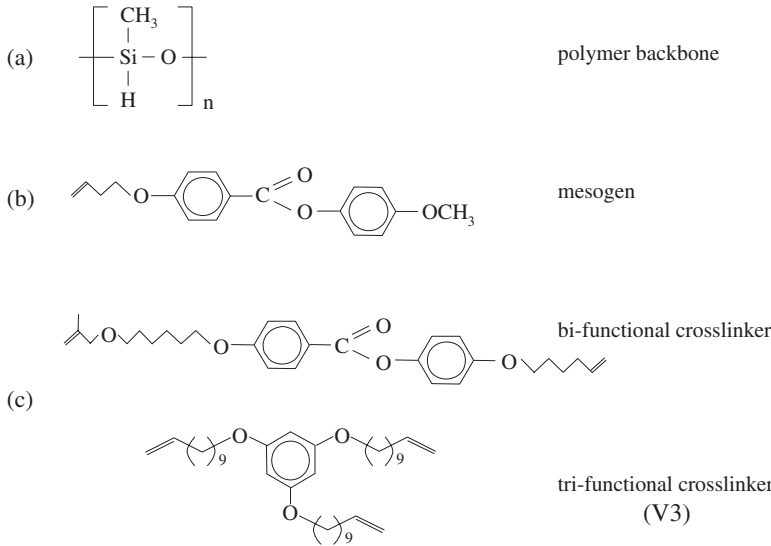


Fig. 1. The chemical structures of the compounds used to prepare the LSCE samples. (a) The methylsiloxane monomer backbone, (b) mesogenic biphenyl side chain, and (c) bi- and tri-functional crosslinkers.

$$\Delta n \propto S. \quad (1)$$

On the other hand, macroscopic strain-deformations  $\varepsilon$  can be introduced as follows:<sup>14,15)</sup>

$$\varepsilon = \frac{1}{\mu}(US - \sigma), \quad (2)$$

where  $\sigma$  is the mechanical stress;  $\mu$ , the elasticity modulus; and  $U$ , the coupling coefficient between  $S$  and  $\varepsilon$ . For  $\sigma = 0$ ,

$$\varepsilon = \frac{U}{\mu}S, \quad (3)$$

i.e.,  $\varepsilon \propto S$ , similar to  $\Delta n$  (see above). In (3), however, no anisotropy is directly taken into account although, in general, one must use an anisotropic generalization of  $\mu$  and  $U$ . Instead, we introduce here the anisotropy of the shape change relative to the director orientation,  $\Delta\alpha$ , which consists of the shrinkage and the expansion components of the  $i = x, y$ , and  $z$  directions. We define  $\Delta\alpha$  as follows (compare ref. 12):

$$\Delta\alpha = \frac{\alpha_x - [\alpha_y + \alpha_z]/2}{\alpha_x + \alpha_y + \alpha_z}. \quad (4)$$

Here,  $\alpha_i(T)$  is the ratio of the length shrinkage/expansion,  $\ell_i(T)$ , to the initial length,  $\ell_i^0$ , in the isotropic phase, parallel to  $\hat{\mathbf{n}}$  ( $\hat{x}$ ) and perpendicular to  $\hat{\mathbf{n}}$  ( $\hat{y}$  and  $\hat{z}$ ); and  $\alpha = 1 + \varepsilon$ . This can be easily shown for linear elasticity and assuming incompressibility, and  $\Delta\alpha$  and the length change parallel to the director used by Küpfer *et al.*<sup>2,3)</sup> are equivalent. Then, we expect the relation  $\Delta\alpha \propto \Delta n$  from (3) and (4).

The temperature dependence of  $\Delta n$  and  $\Delta\alpha$  for dry 8A2, 5V3, and 7V3 samples are shown in Fig. 2.  $\Delta n$  and  $\Delta\alpha$  show a very similar behavior. With increasing temperature,  $\Delta n$  and  $\Delta\alpha$  monotonically decrease for all the samples; the LSCEs shrank parallel to  $\hat{\mathbf{n}}$  ( $\hat{x}$ ) and expanded perpendicular to  $\hat{\mathbf{n}}$  ( $\hat{y}$  and  $\hat{z}$ ),<sup>10–12)</sup> with a slightly faster decrease in the vicinity of  $T_c^{8A2} \sim 80^\circ\text{C}$ ,  $T_c^{5V3} \sim 72^\circ\text{C}$ , and  $T_c^{7V3} \sim 65^\circ\text{C}$  for the 8A2, 5V3, and 7V3 samples, respectively. The  $\Delta n(T)$  and  $\Delta\alpha(T)$  plots exhibit a foot slightly above  $T_c$ . This foot is typical for LSCE samples, i.e., LSCEs typically do not have a direct transition from a nematic to a completely isotropic phase due to the frozen order near cross-linking points.<sup>2,3,9)</sup>

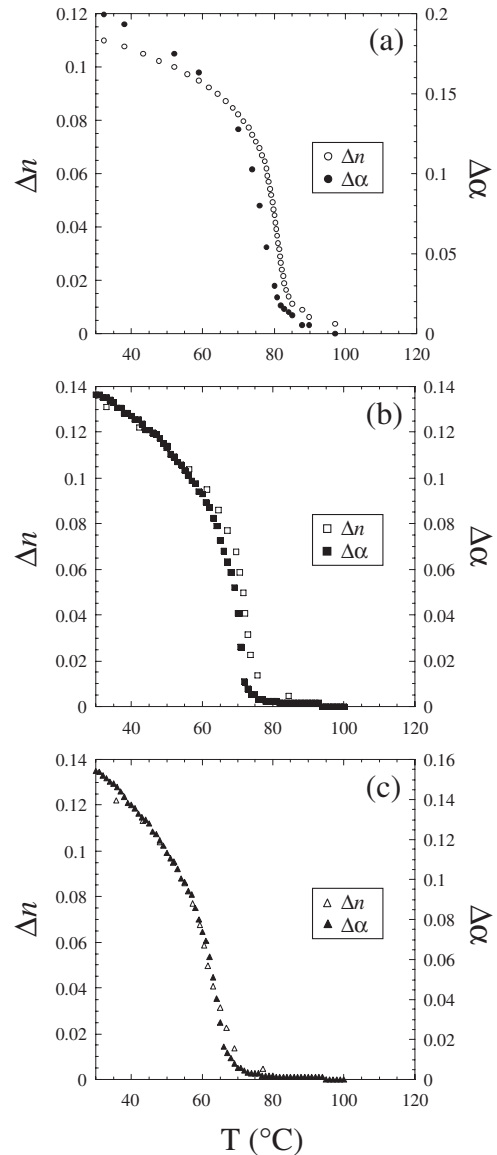


Fig. 2. Temperature dependence of  $\Delta n(T)$  and  $\Delta\alpha(T)$  for dry 8A2 (a), V3LSCE-5 (b), and V3LSCE-7 (c) samples.

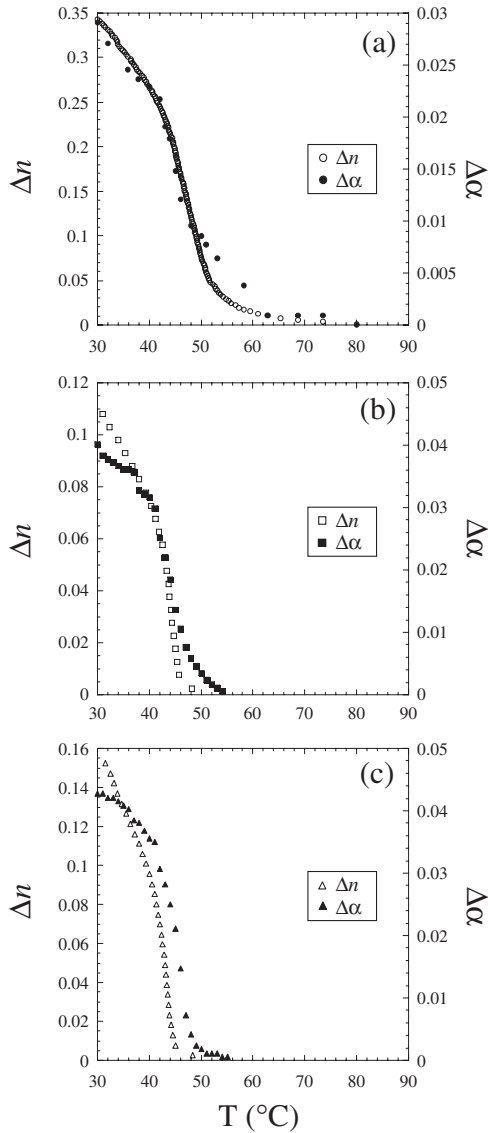


Fig. 3. Temperature dependence of  $\Delta n$  and  $\Delta\alpha$  for swollen 8A2(a), 5V3 (b), and 7V3 (c) samples.

The flexible tri-functional cross-linker is more isotropic-like, as shown in Fig. 1, while the rigid bi-functional cross-linker is more strongly anisotropic. Therefore, 8A2 has more FOO than V3LSCEs (5V3 and 7V3). In V3LSCE samples, the presence of a higher concentration of cross-linking points appears to reduce the degree of nematic order by increasing the disorder and/or by reducing the nematogenic tendencies. Increasing the cross-linking concentration in V3LSCEs will thus favor the isotropic state of the system and reduce the nematic-isotropic phase transition temperature  $T_c$ . The stronger FOO also shows a more pronounced foot in  $\Delta n(T)$  and  $\Delta\alpha(T)$ , as shown in Fig. 2(a).

The two factors influencing the shape anisotropy,  $\Delta\alpha(T)$ , are (1) the network modulus elasticity and (2) FOO. The higher modulus elasticity and FOO, the larger  $\Delta\alpha(T)$ . Increasing the concentration of the tri-functional cross-linkers in V3LSCE materials increases the network modulus, but its isotropy reduces the FOO. Well inside the nematic phase ( $T = 30^\circ\text{C}$ ),  $\Delta\alpha^{8A2} \sim 0.2$ ,  $\Delta\alpha^{5V3} \sim 0.14$ , and  $\Delta\alpha^{7V3} \sim 0.16$ . 8A2 has a larger  $\Delta\alpha(T)$  than that of the V3LSCE samples due to a larger amount of FOO, i.e., more

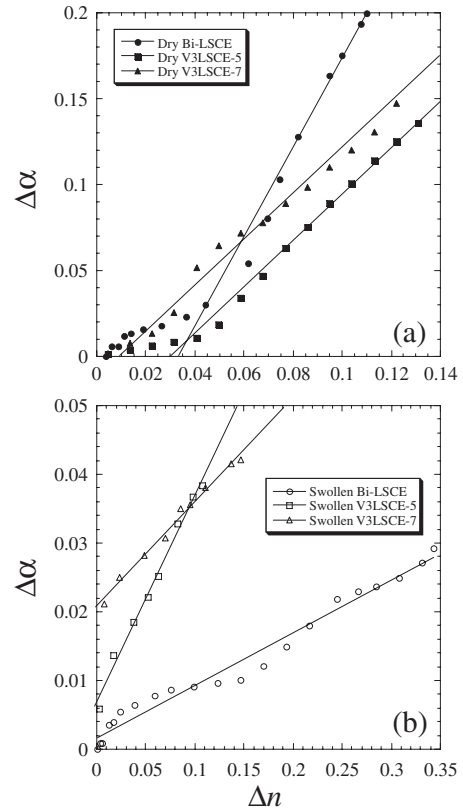


Fig. 4. The shape anisotropy,  $\Delta\alpha$ , is plotted as a function of the optical birefringence,  $\Delta n$ , for dry (a) and swollen (b) samples,  $\Delta\alpha = a + b\Delta n$ . The slope  $b$  for dry samples is about 2.7 for 8A2, 1.4 for 5V3, and 1.1 for 7V3. For swollen samples,  $b$  is about 0.07 for 8A2, 0.3 for 5V3, and 0.15 for 7V3. In (a), the straight lines plotted are obtained as a fit to the data well within the nematic phase, i.e., with  $\Delta n \geq 0.04$ . The direct proportionality between  $\Delta n$  and  $\Delta\alpha$  shows that  $\Delta\alpha$  is directly proportional to the degree of nematic order in LSCEs.

orientational order is stored in 8A2 due to a more anisotropic cross-linker. At  $T = 30^\circ\text{C}$ , the optical birefringence  $\Delta n$  value is around 0.11–0.13 (Fig. 2).

Figure 3 shows  $\Delta n$  and  $\Delta\alpha$  as a function of temperature for the swollen 8A2 [Fig. 3(a)], 5V3 [Fig. 3(b)], and 7V3 [Fig. 3(c)] samples. The maximum value of  $\Delta\alpha$  at  $T = 30^\circ\text{C}$  is about 0.03 for 8A2, 0.04 for 5V3 and 7V3 samples. In the swollen LSCEs, relatively smaller length variations are observed;  $\Delta\alpha$  is reduced substantially by swelling because of the weaker modulus elasticity due to the large amount of 5CB (more than 300%) within the sample, i.e., swelling reduces the elastic modulus.

The changes in  $\Delta n$  for V3LSCEs between dry and swollen samples are small ( $\sim 25\%$ ). However,  $\Delta n$  in the swollen 8A2 is almost a factor of 3 higher than in the dry one and almost a factor of 2 higher than in pure 5CB.<sup>16</sup> This demonstrates that when the FOO is large in the nematic phase of an LSCE, it can lead to a substantial enhancement in the orientational order of the low molecular weight material (5CB), thereby leading to the overall birefringence of the swollen material.

In Fig. 4, when  $\Delta\alpha$  is plotted as a function of  $\Delta n$ , a linear dependence is observed for all LSCE samples, which is well described by eqs. (1) and (3). In dry LSCEs, a linear dependence is observed throughout the nematic phase except for a small region close to  $T_c$ . This can be explained

by the fact that the changes in the shape anisotropy  $\Delta\alpha$  in both the dry and the swollen LSCEs are caused by order parameter changes. However, the magnitude of  $\Delta\alpha$  and  $\Delta n$  depends on the concentration and the functionality of the cross-linkers.

The slope of the dry 8A2 ( $b \sim 2.7$ ) sample is larger than that of the dry 5V3 (1.4) and 7V3 (1.1) samples. This means that the dry 8A2 sample has a larger thermo-mechanical effect than those of the V3LSCEs. However, after swelling with LMWLC, its slope ( $b \sim 0.07$ ) was smaller than that of the V3LSCE samples; the swollen 8A2 is less sensitive to temperature variations. The slope of 5V3 ( $b \sim 0.3$ ) is larger than that of 7V3 (0.15) for both dry and swollen samples. It is inferred that the smaller cross-linking density in swollen V3LSCE is more sensitive to thermo-mechanical effects. In fact, the swelling rate of 8V2 ( $q^{8V2} = 3.2$ ) is also smaller than that of 5V3 ( $q^{5V3} = 4.5$ ) and 7V3 ( $q^{7V3} = 3.8$ ),<sup>11,13</sup> and the swelling rate of 5V3 is larger than that of 7V3. It shows that a correlation exists between the slope and the swelling rate in the swollen LSCEs.

Finally, we wish to address the physical reasons for the nonzero intercepts,  $a$ , in Fig. 4. The relation  $\Delta\alpha \propto \Delta n$  is valid well within the nematic phase. The orientational order of the LC elastomers has several components. The first component is the frozen-in orientational order of LSCEs. The second one is the usual quadrupolar order of nematic elastomers. Finally, there exists the orientational order of LMWLC for the swollen samples. The foot clearly seen in Fig. 2 is due to FOO. For the swollen samples, birefringence of the LMWLC dominates  $\Delta n$  deep within the nematic phase. It becomes zero at the enhanced LMWLC transition temperature to the isotropic state leaving behind only FOO.

We have discussed the shape anisotropy changes and the optical properties of dry and swollen bi-functional cross-linked and tri-functional cross-linked LSCEs as a function of temperature. We have shown that the shape anisotropy,  $\Delta\alpha$ , and the optical birefringence,  $\Delta n$ , are linearly related in all the LSCE samples. This shows that the macroscopic deformations of the dry and swollen LSCEs as a function of temperature are caused by the order parameter changes of LSCEs. The largest  $\Delta\alpha$  ( $\sim 0.2$  at  $T = 30^\circ\text{C}$ ) is found in dry bi-functional cross-linked LSCE (8A2), which has the largest frozen-in orientational order (FOO). The swollen samples show a much smaller  $\Delta\alpha$ ,  $\sim 0.03$ – $0.05$ , because of the resulting smaller modulus elasticity after the swelling process.

## Acknowledgements

We thank Nicole Assfalg and Elke Stibal-Fischer for sending us some of the samples used in these measurements. P. E. Cladis thanks the Alexander von Humboldt-Foundation and the Japan Society for the Promotion of Science (JSPS) for encouragement and support. This work is partially supported by the Japan–Germany Scientific Cooperative Program of JSPS and the Deutsche Forschungsgemeinschaft, the Grant for Scientific Research sponsored by JSPS, and the Grant-in-Aid for Scientific Research on priority areas, No. 438 “Next-Generation Actuators Leading Breakthroughs”. H. R. Brand thanks the Deutsche Forschungsgemeinschaft for partial support of his work through the Forschergruppe FOR 608 “Nichtlineare Dynamik komplexer Kontinua”. Y. Yusuf thanks the Research Fellowships of JSPS.

- 1) H. Finkelmann, H. J. Kock, and G. Rehage: *Makromol. Chem., Rapid Commun.* **2** (1981) 317.
- 2) J. Küpfer and H. Finkelmann: *Makromol. Chem., Rapid Commun.* **12** (1991) 717.
- 3) J. Küpfer and H. Finkelmann: *Makromol. Chem. Phys.* **195** (1994) 1353.
- 4) F. J. Davis and G. R. Mitchell: *Polymer* **37** (1996) 1345.
- 5) I. Kundler and H. Finkelmann: *Macromol. Chem. Phys.* **199** (1998) 677.
- 6) M. Warner and E. M. Terentjev: *Liquid Crystal Elastomers* (Oxford University Press, 2003).
- 7) P. G. de Gennes, M. Hébert, and R. Kant: *Macromol. Symp.* **113** (1997) 39.
- 8) M. Hébert, R. Kant, and P. G. de Gennes: *J. Phys. I* **7** (1997) 909.
- 9) H. R. Brand and K. Kawasaki: *Macromol., Rapid Commun.* **15** (1994) 251.
- 10) Y. Yusuf, P. E. Cladis, H. R. Brand, H. Finkelmann, and S. Kai: *Chem. Phys. Lett.* **389** (2004) 443.
- 11) Y. Yusuf, Y. Ono, Y. Sumisaki, P. E. Cladis, H. R. Brand, H. Finkelmann, and S. Kai: *Phys. Rev. E* **69** (2004) 021710.
- 12) D. U. Cho, Y. Yusuf, P. E. Cladis, H. R. Brand, H. Finkelmann, and S. Kai: *Chem. Phys. Lett.* **418** (2006) 217.
- 13) D. U. Cho, Y. Yusuf, P. E. Cladis, H. R. Brand, H. Finkelmann, and S. Kai: *Jpn. J. Appl. Phys.* **46** (2007) 1106.
- 14) W. Kaufhold, H. Finkelmann, and H. R. Brand: *Makromol. Chem.* **192** (1991) 2555.
- 15) H. Wermter and H. Finkelmann: *e-Polymers* 2001, No. 013 (<http://www.e-polymers.org>).
- 16) S.-T. Wu, C. S. Wu, W. Warengem, and M. Ismaili: *Proc. SPIE* **1815** (1992) 179; compare also G. Pelzl: in *Handbook of Liquid Crystals*, ed. D. Demus, J. Goodby, G. W. Gray, H.-W. Spiess, and V. Vill (Wiley-VCH, Weinheim, 1998) Vol. 2A.